Nonlinear Grey-box Identification of Gravity-driven Sewer Networks with the Backwater Effect

Balla, Krisztian Mark; Knudsen, Casper Houtved; Hodzic, Adis ; Bendtsen, Jan Dimon; Kallesøe, Carsten

Published in:
Nonlinear Grey-box Identification of Gravity-driven Sewer Networks with the Backwater Effect

Publication date:
2021

Document Version
Accepted author manuscript, peer reviewed version

Nonlinear Grey-box Identification of Sewer Networks with the Backwater Effect: An Experimental Study

Krisztian Mark Balla[1,2], *Graduate Student Member, IEEE*, Casper Houtved Knudsen[1], Adis Hodzic[1], Jan Dimon Bendtsen[1], *Member, IEEE*, Carsten Skovmose Kallesøe[1,2], *Member, IEEE*,

***Abstract*— Real-time control of urban drainage networks requires knowledge about stored volumes and flows in order to predict overflows and optimize system operation. However, using flow sensors inside the pipelines means prohibitively high installation and maintenance costs. In this article, we formulate two nonlinear, constrained estimation problems for identifying the open-channel flow in urban drainage networks. To this end, we distribute cost-efficient level sensors along the pipelines and formulate the estimation problems based on the spatially-discretized kinematic and diffusion wave approximations of the full Saint-Venant partial differential equations. To evaluate the capabilities of the two models, the two approaches are compared and evaluated on modeling a typical phenomenon occurring in drainage systems: the backwater effect. An extensive real-world experiment demonstrates the effectiveness of the two approaches in obtaining the model parameters on a scaled water laboratory setup, in the presence of measurement noise.**

I. INTRODUCTION

Urban Drainage Networks (UDNs) are large-scale systems where sewage is transported in open-channel conduits towards the root of the network, where it is treated before being discharged to the environment. In this article, we focus on pumped systems where the sewage is pumped to overcome the elevation and levelness of the landscape, then allowed to flow by gravity towards the next collection pit in line [1]. In order to control the volumes in UDNs, the flows and stored volumes are essential to know to schedule unavoidable overflows and regulate the inlet to the treatment plant [2].

Transport in UDNs is a complex process due to its nonlinear nature and to the large time-delays imposed by long travel times between wastewater pumping stations. The transport processes are modeled by Partial Differential Equations (PDEs), where the level and flow of water appear as independent variables. However, these PDEs are often too complex to solve in real-time applications and require the precise network dimensions or a High Fidelity (HiFi) model of the UDN [3], [4].

Some papers report on using the full dynamic PDEs in control of UDNs [5] and modeling of open-channel water infrastructures, e.g., irrigation canals and river systems. However, using full-PDE models requires a HiFi simulator or installing several flow sensors along the pipelines, resulting in high installation and maintenance costs. To overcome the difficulties with model complexity, some research proposes to use reduced sewer models, relying on the physical attributes (pipe dimensions, friction, slope) of sewer pipes [6]. The most common approximations of the original PDEs are the Kinematic Wave (KW) and Diffusion Wave (DW) methods [7], where the original model is simplified by omitting several physical phenomena in the model [8]. The most common phenomena of this type is the backwater effect, which is a local flow reversal that occurs inside the pipelines when the capacity is overloaded and water volumes are accumulating [4].

Linearizing PDEs around operating points has been extensively used in slowly-varying water applications such as river control, but also in UDNs by means of transfer functions capturing the backwater effect in [9], and by state-space models in [10]. Furthermore, due to its simplicity, delay-models have been used in predictive control in many UDN applications as well [11]. Data-driven modelling has been reported in [12] and [13], where KW approximation-based, grey-box modelling and black-box approaches have been extensively used to model the gravity-driven sewer flows.

In this article, experiments are carried out for both the KW and DW approximations of the full PDEs to compare the model performance in system identification. In contrast to methods relying on flow measurements and HiFi models, we consider level sensors distributed along the network and utilize flow estimation techniques to show the identifiability of the KW- and DW-based models. Our approach is data-driven, yet the models rely on the hydraulics of the network, familiar to operators in the open-channel, water infrastructures industry. Furthermore, the proposed technique using the physically-based process models carries an advantage that it only requires data collection under nominal operation, unlike conventional data-driven methods.

The remainder of the paper is structured as follows. Section II introduces the KW and DW approximation principles of the original PDEs. In Section III, we formulate the system identification problem for both cases, whereupon Section IV describes the case study laboratory setup. The results are provided in Section V, where sensor and estimation data from the experiments are utilized. This is followed by Section VI, where conclusions and future research directions are provided.

a) *Nomenclature:* Throughout the paper, all quantities mentioned are real values. Boldface letters are used for sets, such as $\mathbf{s} = \{s_1, ...s_n\}$ as well as for vectors $\mathbf{x} =$

[1] Section for Automation and Control, Department of Electronic Systems, Aalborg University, Fredrik Bajers vej 7c, DK-9220 Aalborg, Denmark, Email: {kmb,dimon,csk}@es.aau.dk, {ckn16,ahodi19}@student.aau.dk

[2] Technology Innovation, Controls Department , Grundfos Holding A/S, Poul Due Jensens vej 7, DK-8850 Bjerringbro, Denmark, Email: {kballa,ckallesoe}@grundfos.com

$(x_1, ...x_n)^\intercal \in \mathbb{R}^n$. In case of vectors, $<, \leq, =, >, \geq$ denote element-wise relations. Moreover, for a vector $\boldsymbol{x} \in \mathbb{R}^n$, $||\boldsymbol{x}|| = \sqrt{\boldsymbol{x}^\intercal \boldsymbol{x}}$ denotes the Euclidean norm.

II. MODELING

Open-channel flow in UDNs is typically modelled by the shallow water equations, which are given in uni-directional form by the Saint-Venant (SV) PDEs [1]. These PDEs describe the mass balance and the momentum conservation of the fluid, shown in (1a) and (1b), respectively:

$$\frac{\partial A_{x,t}}{\partial t} + \frac{\partial q_{x,t}}{\partial x} = \tilde{d}_{x,t}, \tag{1a}$$

$$\frac{1}{gA_{x,t}}\left(\frac{\partial q_{x,t}}{\partial t} + \frac{\partial}{\partial x}\left(\frac{q_{x,t}^2}{A_{x,t}}\right)\right) + \underbrace{\frac{\partial h_{x,t}}{\partial x} + \overbrace{S_{f|x,t} - S_b}^{\text{Kinematic wave}}}_{\text{Diffusion wave}} = 0, \tag{1b}$$

where $A_{x,t}$ is the wetted area, $q_{x,t}$ is the open-channel flow inside the pipes, $h_{x,t}$ is the water level and $\tilde{d}_{x,t} = d_{x,t}/\delta x$ represent lateral inflows per unit length, where $d_{x,t}$ is the lateral inflow, hereinafter referred to as disturbance. Moreover, all variables mentioned are functions mapping from $(0, L) \times \mathbb{R}_+ \to \mathbb{R}_+$, where L represents the total length of the pipe. The gravity constant is denoted by g and the full dynamic SV-based PDEs are parametrized by the S_b slope and the $S_{f|x,t}$ friction terms. Note, that S_b is independent of the spatial and temporal coordinates, as we assume that the slopes of the modelled pipe segments are close to being constant throughout the pipe length. Moreover, different approximations to the SV-based PDEs exist, depending on which terms are neglected in (1b). In this study, we focus on the Kinematic and Diffusion wave approximations.

Assumption 1: It is assumed that semi-filled pipe segments with a given geometry are sufficiently well-approximated with a rectangular pipe shape. Hence, the wetted area $A_{x,t}$ and perimeter $P_{x,t}$ are approximated as:

$$A_{x,t}(h_{x,t}) \approx w h_{x,t}, \tag{2a}$$

$$P_{x,t}(h_{x,t}) \approx w + 2h_{x,t}, \tag{2b}$$

where w is the width of the pipe. Note, that the accuracy of the linear approximation varies according to the operating level inside the pipes, i.e., how full the pipe segment is.

In the following, the KW and DW reduction of the SV-based PDEs and the geometry simplifications are considered.

A. Kinematic wave approximation

When approximating the full SV-based PDEs with kinematic waves, we assume uniform, quasi-steady flow and neglect the physical phenomena such as the backwater effect by keeping only the $S_{f|x,t}$ friction and S_b slope terms in (1b). Hence, the gravitational and friction forces acting on the fluid are equal.

In order to relate the friction to flows $q_{x,t}$ and water levels $h_{x,t}, x \in (0, L)$, we utilize the Manning formula [14]:

$$S_{f|x,t} = n^2 \frac{P_{x,t}^{4/3}}{A_{x,t}^{10/3}} q_{x,t}^2, \tag{3}$$

where $P_{x,t}$ is the wetted perimeter and n is the Manning friction factor. Using Assumption 1, the friction term in (3) is rewritten as:

$$S_{f|x,t} = n^2 \frac{(w + 2h_{x,t})^{4/3}}{(wh_{x,t})^{10/3}} q_{x,t}^2. \tag{4}$$

Then, isolating $q_{x,t}$ and inserting back into the SV-based PDEs for a square pipe, the KW approximation yields PDEs of first-order in the form:

$$w\frac{\partial h_{x,t}}{\partial t} + \frac{\partial q_{x,t}}{\partial x} = \frac{d_{x,t}}{\delta x}, \tag{5a}$$

$$q_{x,t} = \frac{\sqrt{S_b}}{n} \frac{(wh_{x,t})^{5/3}}{(2h_{x,t} + w)^{2/3}}. \tag{5b}$$

Note that $q_{x,t}$ only depends on $h_{x,t}$, implying that the mapping from level to flow is injective.

To obtain a model structure more amenable to system identification, the PDEs in (5a) and (5b) are reduced to a system of finite-dimensional Ordinary Differential Equations (ODEs) by discretizing each pipe spatially as shown in Fig. 1.

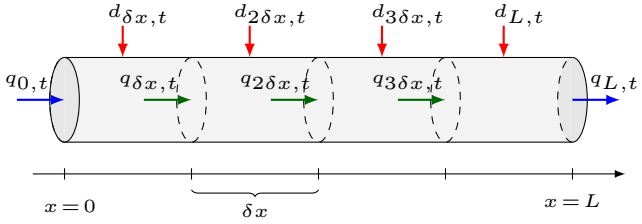

Fig. 1. Flow balances for a pipe discretized into $N_x = 4$ sections.

Note that for each segment, the flow balance incorporates the lateral inflows $d_{x,t}$, the boundary flows $q_{0,t}$, the discharge flow $q_{L,t}$ and the section flows $q_{x,t}$. The section flows are generated by the water level in each pipe segment.

For the spatial discretization, we apply the backward Euler method with a spatial step size of δx, such that:

$$\frac{dh_{x,t}}{dt} = \theta_1(q_{x-\delta x,t} - q_{x,t} + d_{x,t}), \tag{6a}$$

$$q_{x,t} = \theta_2 f(h_{x,t}, \theta_3), \tag{6b}$$

where the nonlinear map $f : \mathbb{R}_+ \to \mathbb{R}_+$ is given by:

$$f : (h_{x,t}, \theta_3) \mapsto \frac{h_{x,t}^{5/3}}{(h_{x,t} + \theta_3)^{2/3}}, \quad \forall\, x \in (0, L), \tag{7}$$

and the physical constants along with the spatial step δx are gathered in parameters, where:

$$\theta_1 \triangleq \frac{1}{w\delta x}, \quad \theta_2 \triangleq \frac{\sqrt{S_b} w^{5/3}}{2^{2/3} n}, \quad \theta_3 \triangleq \frac{w}{2}. \tag{8}$$

Note that the parameters $\theta_1, \theta_2, \theta_3$ are positive, given that the physical constants and the spatial steps are positive.

In order to obtain a model with water levels as states, the $q_{x,t}$ flows in (6a) are substituted with water levels from (6b). For ease of notation the time index t is omitted. Then, the

reduced KW-based model is given by a set of N_x ODEs, each representing a section of length of the pipe:

$$\frac{dh_1}{dt} = \theta_1(q_0 + d_1) - \theta_1\theta_2 f(h_1, \theta_3), \tag{9a}$$

$$\vdots$$

$$\frac{dh_n}{dt} = \theta_1 d_n + \theta_1\theta_2\big(f(h_{n-1}, \theta_3) - f(h_n, \theta_3)\big), \tag{9b}$$

$$\vdots$$

$$\frac{dh_{N_x}}{dt} = \theta_1(d_{N_x} - q_{N_x}) + \theta_1\theta_2 f(h_{N_x-1}, \theta_3), \tag{9c}$$

where the flow q_0 at $x = 0$ is considered as a controlled input. As the section flows depend only on the water levels in the corresponding segments, the discharged flow is calculated directly from the level in the last segment:

$$q_{N_x} = \theta_2 f(h_{N_x}, \theta_3), \tag{10}$$

where h_{N_x} is the water level in the last pipe segment.

B. Diffusion wave approximation

Unlike the KW-based model, the DW approximation does not neglect the term $\partial h_{x,t}/\partial x$ in (1b). Hence, the momentum equation of the SV-based PDEs becomes:

$$\frac{\partial h_{x,t}}{\partial x} = S_b - S_{f|x,t}. \tag{11}$$

In case of the DW approximation, the friction term is given by the open-channel Darcy-Weisbach formula [1]:

$$S_{f|x,t} = k\frac{P_{x,t}}{8A_{x,t}^3 g}q_{x,t}^2, \tag{12}$$

where k is the Darcy-Weisbach friction factor and g is the gravitational acceleration.

To show the structure of the DW-based model, first we spatially discretize the SV-based PDEs in (1). We use the backward Euler method for discretizing $\partial q_{x,t}/\partial x$ in (1a) (as for the KW-based model) and the forward Euler method for $\partial h_{x,t}/\partial x$ in (1b). Then, the SV-based PDEs are reduced to a system of finite-dimensional, first-order ODEs:

$$\delta x w\frac{dh_{x,t}}{dt} = q_{x-\delta x,t} - q_{x,t} + d_{x,t}, \tag{13a}$$

$$h_{x+\delta x,t} - h_{x,t} = z - r(q_{x,t}, h_{x,t}), \tag{13b}$$

where $z \triangleq \delta x S_b$ defines the elevation difference between the equal-sized, non-overlapping segments δx and the pipe resistance $r_x(q_{x,t}, h_{x,t}) \triangleq \delta x S_{f|x,t}$ due to friction. Applying Assumption 1, the resistance function becomes:

$$r_x(q_{x,t}, h_{x,t}) = k\frac{\delta x}{8g}\frac{w + 2h_{x,t}}{w^3 h_{x,t}^3}q_{x,t}^2. \tag{14}$$

The flows $q_{x,t}$ between pipe segments are expressed similarly to the section flows in the KW-based model. The inverse of the resistance function $r(q_{x,t}, h_{x,t})$ is used to solve the momentum equation in (13b), such that:

$$q_{x,t} = r_x^{-1}(h_{x,t} + z - h_{x+\delta x,t}). \tag{15}$$

As opposed to the KW-based model, the pipe flows $q_{x,t}$ are not only a function of the local water levels $h_{x,t}$, but also the water level one spatial step forward and the elevation between the neighboring sections, as depicted in Fig. 2.

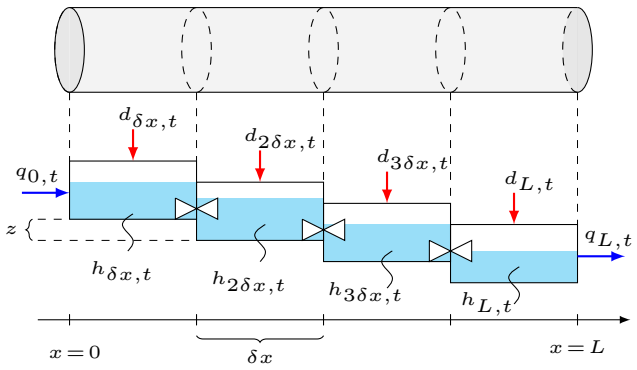

Fig. 2. Discretized pipe, indicating level differences generating the flow.

Note that the relation between section flows $q_{x,t}$ and water levels $h_{x,t}$ is not one-to-one, as it was in the KW-based model. Furthermore, the section flows are generated by the elevation difference due to the pipe slope, as well as by the level difference between the interconnected segments.

The spatial discretization of the DW-based model yields:

$$\frac{dh_{x,t}}{dt} = \lambda_1(q_{x-\delta x,t} - q_{x,t} + d_{x,t}), \tag{16a}$$

$$q_{x,t} = \lambda_2\big((h_{x,t} + z - h_{x-\delta x,t})g(h_{x,t}, \lambda_3)\big)^{1/2}, \tag{16b}$$

where the nonlinear map $g : \mathbb{R}_+ \to \mathbb{R}_+$ is given by:

$$g : (h_{x,t}, \lambda_3) \mapsto \frac{h_{x,t}^3}{h_{x,t} + \lambda_3}, \quad \forall\, x \in (0, L). \tag{17}$$

Here, z is an extra model parameter and the physical constants are collected in parameters, where:

$$\lambda_1 \triangleq \frac{1}{w\delta x}, \quad \lambda_2 \triangleq \left(\frac{4gw^3}{k\delta x}\right)^{1/2}, \quad \lambda_3 \triangleq \frac{w}{2}. \tag{18}$$

Similarly to the KW-based model, the parameters $\lambda_1, \lambda_2, \lambda_3 \in \mathbb{R}_+$. Note that the parameters for the KW and DW case only differ in θ_2 and λ_2.

To obtain a model with water levels as states, the $q_{x,t}$ flows in (16a) are substituted with water levels from (16b). For ease of notation the time index t is omitted. Then, the reduced DW-based model is given by a set of N_x ODEs, each representing a section of length of the pipeline:

$$\frac{dh_1}{dt} = \lambda_1(q_0 + d_1) - \lambda_1\lambda_2\big((h_1 - h_2 + z)g(h_1, \lambda_3)\big)^{\frac{1}{2}}, \tag{19a}$$

$$\vdots$$

$$\frac{dh_n}{dt} = \lambda_1 d_n + \lambda_1\lambda_2\Big[\big((h_{n,t} - h_n + z)g(h_{n-1}, \lambda_3)\big)^{\frac{1}{2}} - \big((h_n - h_{n+1} + z)g(h_n, \lambda_3)\big)^{\frac{1}{2}}\Big] \tag{19b}$$

$$\vdots$$

$$\frac{dh_{N_x}}{dt} = \lambda_1(d_{N_x} - q_{N_x}) + \lambda_1\lambda_2\big((h_{N_x-1} - h_{N_x} + z)g(h_{N_x-1}, \lambda_3)\big)^{\frac{1}{2}}, \tag{19c}$$

where in a similar manner to the KW-based model, the boundary flows at the upstream and downstream end of the

channel are given by q_0 and q_{N_x}, respectively. Unlike the KW-based model, the boundary flow downstream cannot be directly calculated from the water level in the last segment. The DW-based model inherently incorporates the internal connections between the connected elements at the N_x and N_{x+1} spatial steps, where N_{x+1} corresponds to the connected structure.

Remark 1: Hydraulic structures define the level-flow relation at the boundary points of pipelines. These structures are typically wastewater basins, weirs, gates or the receiving water body, e.g., the sea.

The mathematical description of hydraulic structures differs for free [15] and submerged flow [4], hence the model structure and parameters differ too. The outflow-level relation for the two different cases are given by the function:

$$q_{N_x} = G_{\boldsymbol{\mu}_f}(h_{N_x}) \quad \text{for free flow} \tag{20a}$$

$$q_{N_x} = G_{\boldsymbol{\mu}_s}(h_{N_x}, h_{N_x+1}) \quad \text{for submerged flow} \tag{20b}$$

where h_{N_x} is the water level in the last segment of the pipeline and h_{N_x+1} in the hydraulic structure. Moreover, $\boldsymbol{\mu}_f$ and $\boldsymbol{\mu}_s$ are vectors of structure parameters corresponding to free and submerged flows, respectively. Models of hydraulic structures corresponding to the most common elements in UDNs are reported in [4].

C. Discrete system model

In this study, discrete-time system dynamics are utilized for solving the system identification problems for both the KW- and DW-based models. The dynamics of the KW-based model described in (9) and (10) are given for one pipeline:

$$\hat{\boldsymbol{h}}(t_{k+1}) = \boldsymbol{F}_{\boldsymbol{\theta}}^{\text{KW}}\big(\hat{\boldsymbol{h}}(t_k), q_0(t_k), \boldsymbol{d}(t_k)\big), \tag{21a}$$

$$q_{N_x}(t_k) = \theta_2 f(h_{N_x}(t_k), \theta_3), \tag{21b}$$

where the numerical integration from t_k to t_{k+1} is done by the fixed-step 4$^{\text{th}}$ order Runge-Kutta method. Furthermore, $\hat{\boldsymbol{h}}(t_k) \in \mathbb{R}^{N_x}$ is the vector of states, representing the water levels in each of the N_x sections. The vector $\boldsymbol{d}(t_k)$ represents lateral inflow disturbances along the pipe line in each segment. The dynamics are given by $\boldsymbol{F}_{\boldsymbol{\theta}}^{KW} : \mathbb{R}^{N_x} \times \mathbb{R}_+ \times \mathbb{R}^{N_x} \to \mathbb{R}^{N_x}$. The outlet flows are given by (21b).

The dynamics of the DW-based model described in (19a) are given for one pipeline:

$$\hat{\boldsymbol{h}}(t_{k+1}) = \boldsymbol{F}_{\boldsymbol{\lambda},z}^{\text{DW}}\big(\hat{\boldsymbol{h}}(t_k), q_0(t_k), q_{N_x}(t_k), \boldsymbol{d}(t_k)\big), \tag{22}$$

where the dynamics are given by $\boldsymbol{F}_{\boldsymbol{\lambda},z}^{DW} : \mathbb{R}^{N_x} \times \mathbb{R}_+ \times \mathbb{R}_+ \times \mathbb{R}^{N_x} \to \mathbb{R}^{N_x}$. The discharged flow is given by (20a).

III. SYSTEM IDENTIFICATION

The system identification problem in both cases is given by a finite-dimensional constrained Nonlinear Programming (NLP) problem, where the boundary flows q_0, q_{N_x} and the disturbances $\boldsymbol{d}$ at t_i, $i = \{0, ..., N_t\}$ are known a priori.

Remark 2: The pumped inlet flows are estimated by the polynomial expression of fixed-speed wastewater pumps [16], and the outlet flows are estimated by mass conservation. The flow estimation algorithm suitable for the application and methodologies presented in this study is detailed in [16], which the interested reader may refer to for more details.

Water levels in each sections of the gravity pipe are also known a priori by means of sensor measurements, given by:

$$\boldsymbol{v} = \boldsymbol{C}\boldsymbol{h} + \nu, \tag{23}$$

where $\boldsymbol{C} \in \mathbb{R}^{N_0 \times N_x}$ is picking out all measured states $\boldsymbol{v}$ from the states $\boldsymbol{h}$. N_0 denotes the number of level sensors and $\nu \in NID(0, \sigma^2)$ is white Gaussian measurement noise.

The input vector for the KW-based identification at time instance t_i is given by $\boldsymbol{u}(t_i) \triangleq \big(q_0(t_i), \boldsymbol{d}^\intercal(t_i)\big)^\intercal$, and the corresponding output vector by $\boldsymbol{y}(t_i) \triangleq \big(\boldsymbol{v}^\intercal(t_i), q_{N_x}(t_i)\big)^\intercal$. The model parameters are given by $\boldsymbol{\theta} \triangleq (\theta_1, \theta_2, \theta_3)^\intercal$. Then, the NLP problem for the KW-based model is given by:

$$\begin{pmatrix} \boldsymbol{\theta}^* \\ \hat{\boldsymbol{h}}(t_0)^* \end{pmatrix} = \underset{\boldsymbol{\theta}, \hat{\boldsymbol{h}}(t_0)}{\operatorname{argmin}} \sum_{i=0}^{N_t} \big(q_{N_x}(t_i) - \hat{q}_{N_x}(t_i)\big)^2 + \Omega ||\boldsymbol{v}(t_i) - \hat{\boldsymbol{v}}(t_i)||^2 \tag{24a}$$

subject to dynamics in (21) and to inequality constraints:

$$\boldsymbol{0} < \hat{\boldsymbol{h}}(t_i) \leq \overline{\boldsymbol{h}}, \tag{24b}$$

$$0 < \hat{q}_{N_x}(t_i) \leq \overline{q}_{N_x}, \tag{24c}$$

$$\boldsymbol{0} < \boldsymbol{\theta} \leq \overline{\boldsymbol{\theta}}, \tag{24d}$$

where (24b), (24c) and (24d) impose bounds on states, outputs and parameters, respectively. Note that the upper and lower bounds in each constraint are based on meaningful physical values, e.g., the slope and width of the channel must be within meaningful physical ranges and the water levels and flows cannot be negative. Besides, Ω is a weighing constant in (24a), scaling the water levels to flows.

Unlike the KW-based model identification, the inputs in the DW-based model at time instance t_i are defined by $\boldsymbol{u}(t_i) \triangleq \big(q_0(t_i), q_{N_x}(t_i), \boldsymbol{d}^\intercal(t_i)\big)^\intercal$, while the outputs are $\boldsymbol{y}(t_i) \triangleq \big(\boldsymbol{v}^\intercal(t_i)\big)^\intercal$. Furthermore, we define the parameter vector by $\boldsymbol{\lambda} \triangleq (\lambda_1, \lambda_2, \lambda_3)^\intercal$. Note that instead of using the outflow model defined at the downstream boundary of pipelines, described in (20a), the estimated discharged flow q_{N_x} is used as an input. This is done in order to avoid introducing extra μ parameters for hydraulic structures, hence restrict the parameter space. Instead, the flow q_{N_x} is estimated as stated in Remark 2. Then, the NLP problem for the DW-based model is given by:

$$\begin{pmatrix} \boldsymbol{\lambda}^* \\ z^* \\ \hat{\boldsymbol{h}}(t_0)^* \end{pmatrix} = \underset{\boldsymbol{\lambda}, z, \hat{\boldsymbol{h}}(t_0)}{\operatorname{argmin}} \sum_{i=0}^{N_t} ||\boldsymbol{v}(t_i) - \hat{\boldsymbol{v}}(t_i)||^2 \tag{25a}$$

subject to dynamics in (22) and to inequality constraints:

$$\boldsymbol{0} < \hat{\boldsymbol{h}}(t_i) \leq \overline{\boldsymbol{h}}, \tag{25b}$$

$$\boldsymbol{0} < \boldsymbol{\theta} \leq \overline{\boldsymbol{\theta}}, \tag{25c}$$

$$0 < z \leq \overline{z}, \tag{25d}$$

where similarly to the KW case, (25b) imposes bounds on the states, and (25c) and (25d) on the parameters, respectively.

The NLP problems in both cases are solved by using a Gauss-Newton gradient-based method, detailed in [17].

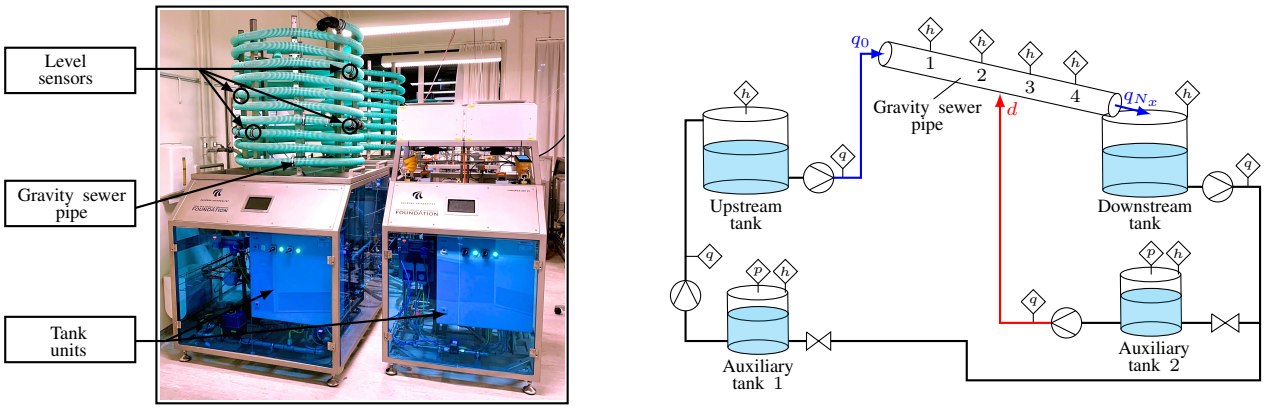

Fig. 3. Sewer modules of the Smart Water Laboratory setup at Aalborg university (left). Schematics of the experimental setup (right). The sensor placements are indicated for each individual module with pressure sensor (p), level sensor (h) and flow sensor (q).

Furthermore, the auxiliary variable N_x, i.e., the number of sections into which each pipeline is discretized into are fixed in both NLP problems. Grid size selection can be evaluated on Monte Carlo simulations for varying step sizes [12].

IV. CASE STUDY

The experimental setup for validating the proposed methodologies is shown in Fig. 3. The setup represents a scaled version of a typical gravity-driven sewer pipeline most commonly found in real-life infrastructures. The proposed setup consists of an open-channel pipeline, along which $N_0 = 4$ level sensors are installed. The inlet flow q_0 is pumped from an upstream tank, while the discharged flow q_{N_x} is calculated from the mass balances of a downstream tank. Auxiliary tanks are utilized as flow sources to pump the disturbance in the middle point of the open-channel sewer pipe. Note, that the disturbance enters the pipeline between the second and third level sensor. Hence, the designed flow event allows to create backflow in the middle of the channel, which is captured by the second level sensor and then propagates to the downstream tank. The level and flow measurement data are obtained and locally managed at each laboratory unit with a Codesys soft-PLC [18], and all local modules are interfaced in real-time. The data used for system identification is gathered over a three-hours long experiment and sampled at $T = 2[s]$. Besides, both the KW and DW models utilized in the system identification are built up of a pipeline discretized into $N_x = 8$ sections.

V. EXPERIMENTAL RESULTS

Following the KW and DW model methodologies discussed in Section II, the two problems have been verified on data extracted from the same experiment. The inlet flow q_0 and lateral inflow d is shown in Fig. 5 (a-b), where the inlet pumps turn on and off with a fixed speed, while there is a consecutive inflow event in the middle of the experiment.

In case of the KW-based model, the output vector $\boldsymbol{y}$ includes the discharged flow q_{N_x}, hence the flow prediction is tested against data. As shown in Fig. 4, the one-step prediction of the KW-based model produces accurate flows compared to the estimated discharge flow data. The validation results show that the model is predicting precisely the flow-dependant process delays both in the presence and without the lateral inflows.

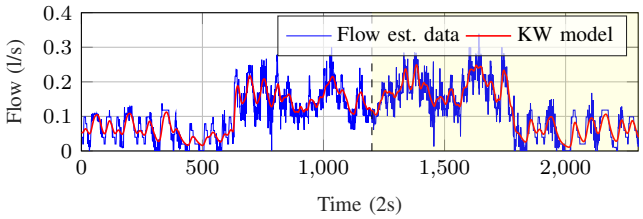

Fig. 4. Identification and validation of discharged flow in the KW model.

Note that the discharged flow increases, when lateral inflow is present along the pipe. This is due to mass conservation, as extra volume is propagating down the channel.

The comparison of the one-step state prediction for the KW- and DW-based models is shown in Fig. 5. Note that the first sensor measurement (h_1) is not affected by the backflow, however, as the disturbance is applied to the system, the sensor at the second position (h_2) captures the water volumes accumulating inside the pipes. This is shown in (e-f), where the KW-based model assumes the downstream propagation of the disturbance without affecting the upstream state, i.e. h_2. In contrast to that, the DW-based model finds the correct z parameters, and due to the level difference in the segments, accounts for the backflow. As shown in Fig. 5 (g-h-i-j), both models are equally good at state prediction after the location where the disturbance enters the channel.

VI. CONCLUSION

In this article, a comparison of two model structures reduced from the Saint-Venant partial differential equations has been presented to model open-channel, gravity-driven flow processes with the backwater phenomena. To this end, a grey-box approach has been proposed using level sensors distributed along the pipeline and utilizing the spatially discretized kinematic and diffusion wave approximations of the full dynamic Saint-Venant equations. The constrained nonlinear system identification problem has been solved for both approaches, where data has been extracted from a scaled laboratory setup built for control of water infrastructures. The experimental results corroborate the feasibility of both approaches and point out the capabilities of the diffusion wave approach in capturing backflow inside the pipes.

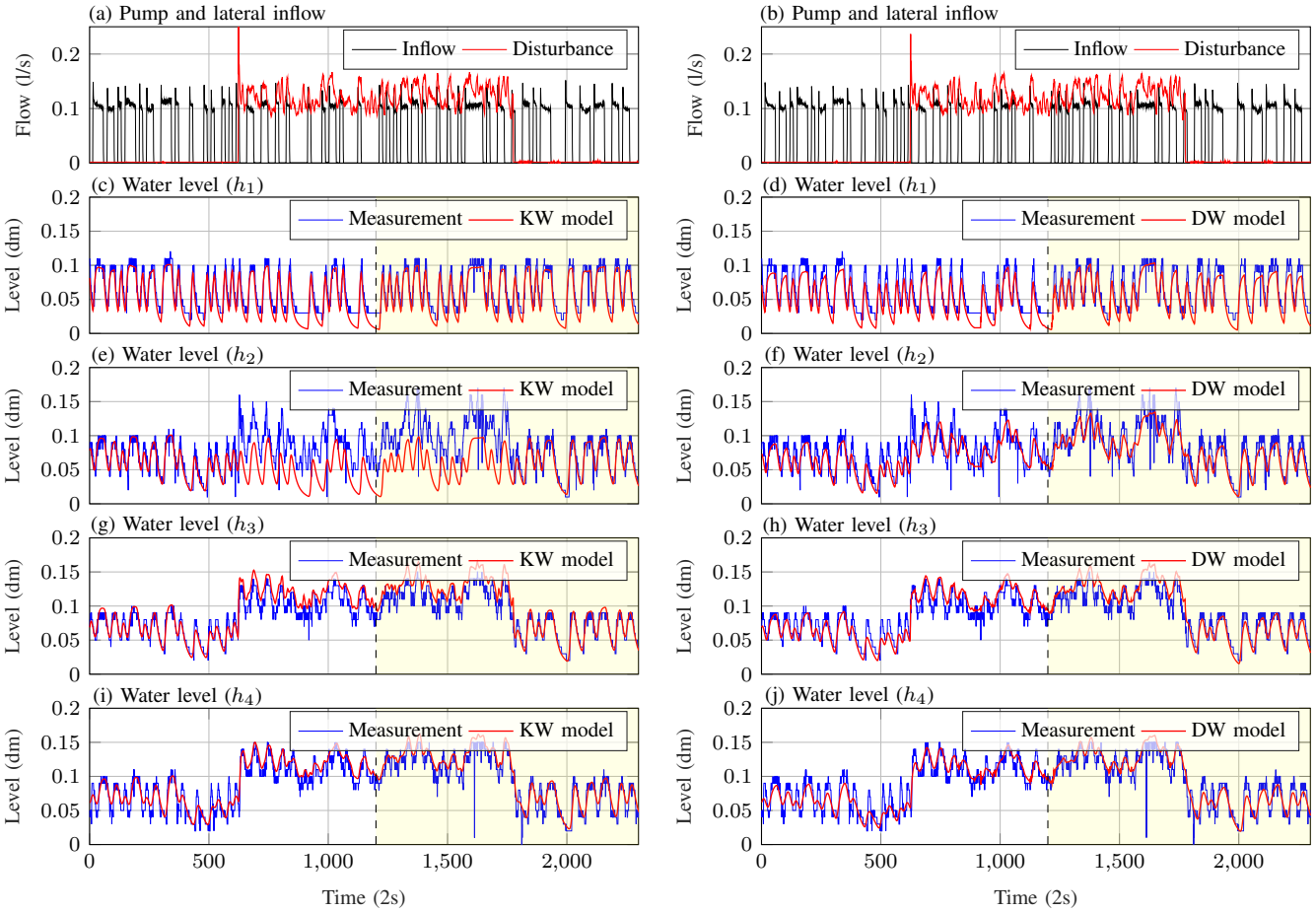

Fig. 5. System identification and validation results for the KW- (left) and the DW-based (right) modelling approaches.

In future work, the two methodologies will be tested on real water infrastructures. Moreover, it will be interesting to carry out stability and identifiability analysis, especially on complex models as the diffusion wave. Applying the methods in predictive control is also a matter of future work.

ACKNOWLEDGMENT

The authors would like to thank the Poul Due Jensen Foundation for providing the Smart Water Lab at Aalborg University. The project was supported by Innovation Fund Denmark and Grundfos Holding A/S as part of a Danish Industrial Ph.D. Project [Application number: *9065-00018A*].

REFERENCES

[1] M. R. Schütze, D. Butler, and M. B. Beck, *Modelling, Simulation and Control of Urban Wastewater Systems*. Springer, 2nd ed., 2002.

[2] M. S. Gelormino and N. L. Ricker, "Model-predictive control of a combined sewer system," *International Journal of Control*, vol. 59, no. 3, pp. 793–816, 1994.

[3] C. Ocampo-Martinez, *Model Predictive Control of Wastewater Systems*. Barcelona: Springer, 1st ed., 2010.

[4] X. Litrico and V. Fromion, *Modeling and control of hydrosystems*. Springer, 2009.

[5] M. Xu, R. R. Negenborn, P. J. van Overloop, and N. C. van de Giesen, "De Saint-Venant equations-based model assessment in model predictive control of open channel flow," *Advances in Water Resources*, vol. 49, no. December, pp. 37–45, 2012.

[6] M. Xu, P. J. van Overloop, and N. C. van de Giesen, "On the study of control effectiveness and computational efficiency of reduced Saint-Venant model in model predictive control of open channel flow," *Advances in Water Resources*, vol. 34, no. 2, pp. 282–290, 2011.

[7] V. P. Singh, "Kinematic wave modelling in water resources: A historical perspective," *Hydrological Processes*, vol. 15, no. 4, pp. 671–706, 2001.

[8] G. Evans, J. Blackledge, and P. Yardley, *Numerical methods for partial differential equations*. Springer Science & Business Media, 2012.

[9] X. Litrico and V. Fromion, "Boundary control of linearized Saint-Venant equations oscillating modes," *Automatica*, vol. 42, pp. 967–972, 2006.

[10] Y. Zou, L. Cen, D. Li, and X. He, "Simplified state-space model and validation of irrigation canal systems," in *Chinese Control Conference, CCC*, (Hangzhou), pp. 2002–2007, 2015.

[11] K. M. Balla, C. Schou, J. D. Bendtsen, and C. S. Kallesoe, "Multi-scenario model predictive control of combined sewer overflows in urban drainage networks," in *4th IEEE Conference on Control Technology and Applications*, (Montreal, Canada), pp. 1042–1047, 2020.

[12] K. M. Balla, C. S. Kallesøe, C. Schou, and J. D. Bendtsen, "Nonlinear Grey-Box Identification with Inflow Decoupling in Gravity Sewers.," in *IFAC 2020 - 21st IFAC World Congress*, (Berlin, Germany), 2020.

[13] S. C. Troutman, N. Schambach, N. G. Love, and B. Kerkez, "An automated toolchain for the data-driven and dynamical modeling of combined sewer systems," *Water Research*, vol. 126, pp. 88–100, 2017.

[14] J. A. Roberson and C. T. Crowe, *Engineering Fluid Mechanics*. Boston: Houghton Mifflin Company, 5th ed., 1993.

[15] S. Dey, "Free overfall in open channels: State-of-the-art review," *Flow Measurement and Instrumentation*, vol. 13, no. 5-6, pp. 247–264, 2002.

[16] C. S. Kallesøe and T. Knudsen, "Self calibrating flow estimation in waste water pumping stations," in *Proceedings of the 2016 European Control Conference (ECC2016)*, (Aalborg), pp. 55–60, 2016.

[17] A. Wills and B. Ninness, "On gradient-based search for multivariable system estimates," *IEEE Transactions on Automatic Control*, vol. 53, no. 1, pp. 298–306, 2008.

[18] 3S-Smart Software Solutions GmbH, "Codesys."